7

Ultrahigh Density Probe-based Storage Using Ferroelectric Thin Films

Noureddine Tayebi[1] and Yuegang Zhang[2]
[1]*Department of Electrical Engineering, Stanford University,*
[2]*The Molecular Foundry, Lawrence Berkeley National Laboratory,*
USA

1. Introduction

The probe-based seek-and-scan data storage system is an ideal candidate for future ultrahigh-density (> 1 Tbit/ inch^2) nonvolatile memory devices (Vettiger et al., 2002; Pantazi et al., 2008; Hamann et al., 2006; Ahn et al., 1997; Cho et al., 2003; Cho et al., 2005; Ahn et al., 2004; Cho et al., 2006; Heck et al., 2010). In such a system, an atomic force microscope (AFM) probe (or an array of AFM probes) is used to write and read data on a nonvolatile medium; the bit size depends mainly on the radius of the probe tip. Moreover, the storage area is not defined by lithography like in SSDs, but rather by the movement of the probes. Thus improving the probe motion control to the tenth of a distance can translate into two orders of magnitude higher density. Bit size as small as 5 nm and a storage density in the Tbit/ in^2 regime with data rate comparable to flash technology have been achieved (Cho et al., 2005; Cho et al., 2006). Unlike SSD technology which requires new lithographic and fabrication tools for each new generation, manufacturing of the probe-based device can be achieved using existing low-cost semiconductor equipment, which can reduce the price of these devices considerably. Another advantage of probe-based memory is that the mechanism to move the probes is low power, which reduces power consumption and heat dissipation in comparison to HDD devices.

While various writing mechanisms have been proposed for probe-based storage, e.g., thermomechanical and thermal writings on polymeric and phase-change media (Vettiger et al., 2002; Pantazi et al., 2008; Hamann et al., 2006), a great deal of attention has recently been devoted to the electrical pulse writing on ferroelectric films due to the non-structure-destructive nature of the write-erase mechanism (Ahn et al., 1997; Cho et al., 2003; Cho et al., 2005; Ahn et al., 2004; Cho et al., 2006; Heck et al., 2010). When a short electrical pulse is applied through a conductive probe on a ferroelectric film, the highly concentrated electric field can invert the polarization of a local film volume, resulting in a nonvolatile ferroelectric domain that is the basis of data recording. This mechanism allows for longer medium lifetime, i.e., larger number of write-erase cycles that is comparable to hard disk drives, faster write and read times (Forrester et al., 2009), smaller bit size (Cho et al. (2006) and higher storage densities (Cho et al. (2006).

Although the probe-based storage technology based on ferroelectric media has shown great promise, no commercial product has yet reached the market. This is mainly due to

fundamental limitations of the media material and probe-media contact during probe-sliding. For ultrahigh storage density exceeding 1 Tbit/ inch^2, domain size reduction below 10 nm is required. Small domain sizes can be obtained by decreasing the size of the probe tip. However, the inverted domain is subjected to ferroelectric depolarization charges and domain-wall energy (Li et al., 2001; Wang & Woo, 2003; Kim et al., 2003) that can be high enough to invert the domain back to its initial polarization. It has been predicted (Wang & Woo, 2003) that inverted ferroelectric domains smaller than 15 nm are unstable and could be inverted back to their initial state as soon as the electric pulse is removed. This instability can be further exacerbated by the presence of a built-in electric field due to film defects present in thin ferroelectric films, which is anti-parallel to the inverted domain polarization. In short, this fundamental instability has prevented the demonstration of stable inverted domains less than 10 nm in size in ferroelectrics. Reading such sub-10 nm inverted domains at the required high speed and with high signal-to-noise ratio (SNR) is also another important issue as such a technique has to be suitable for a MEMS-based probe storage system (Heck et al., 2010).

Another technological bottleneck is that the high data access rate requires a probe-tip sliding velocity on the order of 5 to 10 mm/ s, over a lifetime of 5 to 10 years, corresponding to probe-tip sliding distances of 5 to 10 km. The bit size, and thus the storage density, mainly depends on the radius of the probe-tip that is prone to rapid mechanical wear and dulling due to the high-speed contact mode operation of the system (Cho et al., 2006; Knoll et al., 2006; Bhushan et al., 2008; Gotsmann et al., 2008). This tip wear causes serious degradation of the write-read resolution over the device lifetime.

In this chapter, we review solutions that have been proposed in the literature to address the above fundamental issues and that will enable the development of probe-based nonvolatile memories with storage densities far exceeding those available in today's market. This chapter is divided into four parts. In the first part, the relevant theory and mechanism of pulse-based writing as well as probe-based storage technology on ferroelectric media are reviewed. The stability of single-digit nanometer inverted domains is addressed next. Reading schemes at high frequency and speed are then discussed. Finally a wear endurance mechanism, which allows a conductive platinum-iridium (PtIr) coated probe-tip sliding over a ferroelectric film at a 5 mm/ s velocity to retain its write-read resolution over a 5 km sliding distance, is reviewed.

2. Background

Ferroelectric materials such as $BaTiO_3$ and $Pb(Zr_{0.2}Ti_{0.8})O_3$ (PZT) have a perovskite crystal structure in which the central atom (Ba/ Zr/ Ti) is bi-stable and can be shifted up or down by applying an external electric field (Figure 1a) (Ahn et al., 2004). Upon removal of the external field, the new atom polarization remains, resulting in a nonvolatile property, which is the basis of data recording. To shift the polarization of the central atom, a probe tip can be used (Figure 1b). By contacting the probe tip to the ferroelectric film and applying a bias pulse between them, a highly concentrated electric field underneath the tip is created which flips the polarization of a local volume of atoms and form an inverted polarization domain that can be used as bits for data storage (Figure 1c). The bit can be erased by applying a pulse of a reverse polarity which will switch the polarization within the written domain (Figure 1d) (Cho et al., 2003).

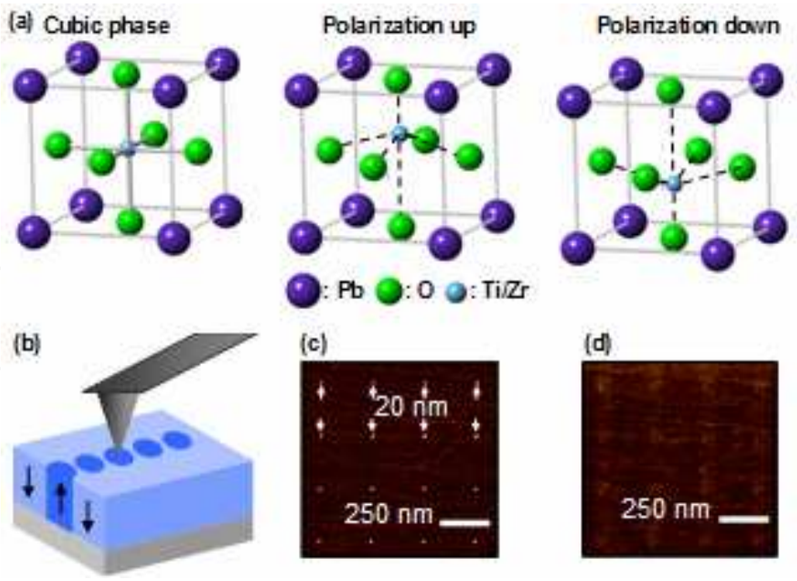

Fig. 1. Data storage on ferroelectric media. (a) Crystal structure of the perovskite ferroelectric PZT showing upward and downward polarization variants. (b) Schematic of bit writing using a probe tip to which a voltage is applied. (c) 4×4 inverted domain dot array formed on a ferroelectric medium. (d) Selective erasing of domain dots by applying a bias of reverse polarity.

The size of the volume mainly depends on the sharpness of the probe tip. In principal, the inverted volume can be as small as an individual atom, and thus allowing for a single atom memory (Ahn et al., 2004). Therefore, an ultrahigh density memory can be constructed with such a system if ultra-sharp probe tips are used and cross talk between bits is avoided. In fact, bit sizes as small as 5 nm (Figure 2a) and a storage density of 10 Tbit/ in^2 with an 8 nm bit spacing have been achieved (Figure 2b) (Cho et al., 2006; Cho et al., 2005). Such a storage density is by far the highest ever achieved in any storage system. Moreover, domain switching times can be as fast as 500 ps, allowing for high writing rate (Figure 2c).

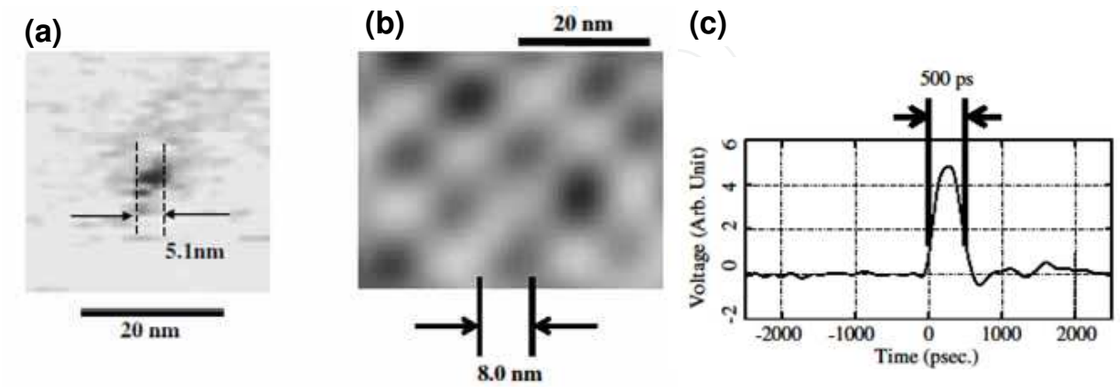

Fig. 2. Nanodomain formed using pulse writing on ferroelectric media. (a) Smallest nanodomain reported in the literature (Cho et al., 2006). (b) Highest writing density ever achieved corresponding to 10 Tbit/ in2 (Cho et al., 2006). (c) 500 ps long pulse used to fully invert nanodomains in ferroelectric media (Cho et al., 2006).

Following the IBM Millipede and HP ARS systems, a joint team at Intel and Nanochip (a startup company) has recently developed a device named "seek-and-scan probe (SSP) memory device" in which the pulse writing scheme using ferroelectric media is used (Heck et al., 2010). The device architecture is shown in Figure 3 and consists of three layers. The bottom layer contains an array of 5000 MEMS cantilevers with tips that are directly fabricated on CMOS circuitry. The cantilevers are spaced at a 150 μm pitch, corresponding to the stroke of the electromagnetically actuated *x–y* micro-mover which forms the second layer of the device with the ferroelectric media film grown on its lower side. The third layer is a cap wafer that seals the device. The device is 15.0×13.7 mm^2 in size and consumes less than 750 mW with a maximum of 5% related to the MEMS actuation. It is capable of achieving a data rate of 20 Mbyte/ s using 272 read-write channels. This rate is the highest ever reported in probe-based devices.

The MEMS cantilevers are fabricated directly on standard Al-backend CMOS in order to increase the overall signal-to-noise ratio (SNR) of the device. This is achieved by growing a low temperature (<455 °C) poly-SiGe film directly on the CMOS circuitry with a thin (5/ 10 nm) Ti/ TiN interfacial layer to provide high contact resistance. This is followed by the deposition of various layers of low temperature oxide and poly-SiGe, which are micromachined to form the various parts of the free standing cantilevers. The probe-tip is defined by depositing a low-stress amorphous Si layer which is subsequently etched using various isotropic and anisotropic etching steps. Detailed fabrication steps of the device can be found in Heck et al, 2010. Figure 4 shows the MEMS cantilever design and SEM images of an individual cantilever. The probe-tips at the end of the cantilevers are brought into contact with the media by electrostatic actuators at the opposite end, which provide both vertical and lateral actuations. The vertical actuation uses a see-saw configuration with an actuation electrode. A torsional beam provides the restoring force. The lateral actuation maintains sub-nanometer positioning of the tip on the data tracks in the presence of non-uniform thermal stresses and macroscale distortion of the device.

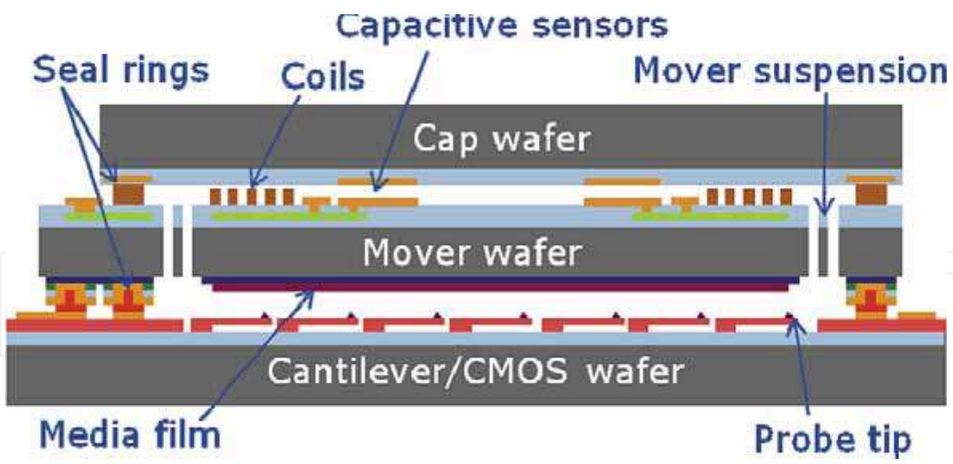

Fig. 3. Schematic of Intel SSP memory device architecture (Heck et al., 2010).

The *x–y* micro-mover is actuated using conductive coils on its top side in the presence of external magnets that reside in recesses in the top of the cap wafer. Micromachined suspension beams allow for high in-plane compliance while maintaining high out-of plane stiffness in order to keep a constant tip-media gap. For position sensing, capacitive sensors are fabricated on the top of the mover and the bottom of the cap. A photograph of the cap – mover assembly is shown Figure 5.

3. Stability of single-digit nanometer domains in ferroelectric films

3.1 Fully inverted ferroelectric domains

For ultra-high storage density exceeding 1 Tbit/ inch^2, domain size reduction below 10 nm is required. Small domain sizes can be obtained by decreasing the size of the probe tip. Unfortunately, the inverted domain is subjected to ferroelectric depolarization charges and domain-wall energy (Li et al., 2001; Wang & Woo, 2003; Kim et al., 2003) that can be high enough to invert the domain back to its initial polarization. It has been predicted (Wang & Woo, 2003) that inverted ferroelectric domains smaller than 15 nm are unstable and could be inverted back to their initial state as soon as the electric pulse is removed. This instability can be further exacerbated by the presence of a built-in electric field due to film defects present in thin ferroelectric films, which is anti-parallel to the inverted domain polarization. In short, this fundamental instability has prevented the demonstration of stable inversion domains less than 10 nm in size in ferroelectrics.

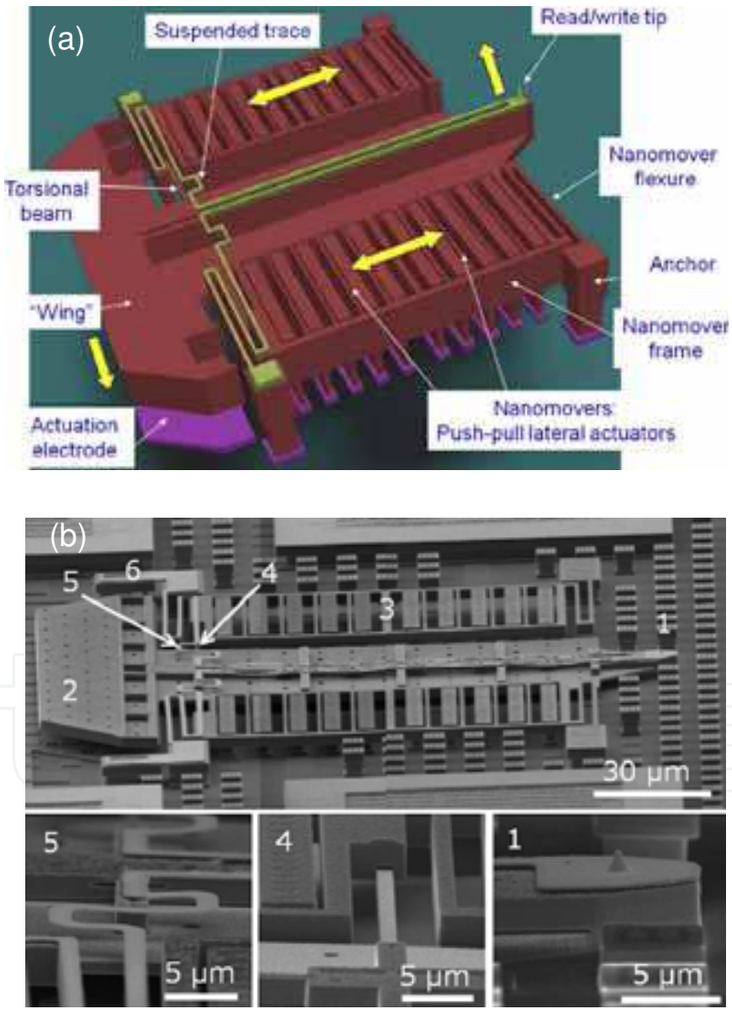

Fig. 4. Intel SSP memory device. (a) Articulated cantilever/ tip design (Heck et al, 2010). (b) SEMs of an individual cantilever with probe-tip. 1: probe tip, 2: vertical actuator called wing, 3: lateral actuators called ''nanomover", 4: torsion beam for vertical actuation, 5: suspended Pt trace, 6: via between trace and CMOS (Heck et al, 2010).

Recently, our group has shown that single-digit nanometer domains remain stable if a critical ratio between probe size and ferroelectric film thickness is reached that would enable full polarization inversion through the entire ferroelectric film thickness (Tayebi et al., 2010a). To obtain reliably and repeatably sub–10 nm inverted domains, we used dielectric sheathed single-walled carbon nanotube (SWNT) prbes termed "nanopencils", which could operate in contact mode while withstanding forces as high as 14.5 μN without bending and buckling (Tayebi et al., 2008).

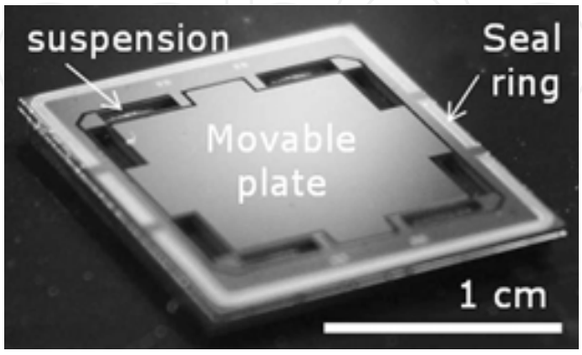

Fig. 5. Photograph of underside of cap/ mover assembly (Heck et al, 2010).

Figures 6a,b show transmission electron microscopy (TEM) images of two nanopencil probes composed of a bundle of a few SWNTs (9 nm overall diameter) and of an individual SWNT (3 nm diameter), respectively. The nanopencils were used to write inverted domain dots on an atomically-smooth, single-crystalline 50-nm-thick ferroelectric PZT film grown on $SrRuO_3$/ $SrTiO_3$(100) substrate using metal-organic chemical vapor deposition (MOCVD) (Tayebi et al., 2008; Tayebi et al, 2010a). The film was initially polarized in an upward direction. Dot sizes as small as 11.8 nm were reliably written with the 9 nm SWNT electrode at 7 V bias pulse (Figure 6c). When trying to write the dots using the 3 nm electrode shown in Figur 6b, however, no domain inversion was recorded even at 10 Vbias pulse (Figure 6d).

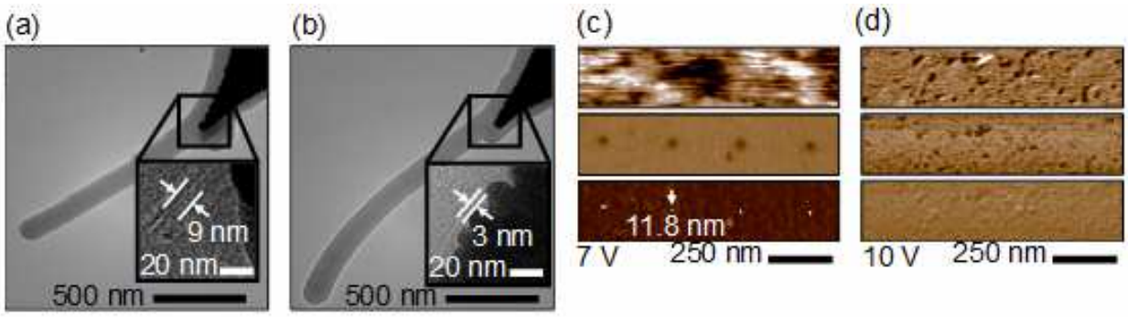

Fig. 6. SWNT-based nanopencil probe for ultra-high density probe-based storage (Tayebi et al., 2010a). (a) and (b) Transmission electron microscopy (TEM) images of nanopencil probes composed of a bundle of a few SWNTs with 9 nm overall diameter (a) and an individual SWNT with 3 nm diameter (b). (c) PFM height (top), amplitude (middle) and phase (bottom) images of a 50nm-thick PZT-film surface with 11.8 nm ferroelectric inverted domains formed by applying 7 V pulses to the film through the nanopencil shown in (a). (d) PFM height (top), amplitude (middle) and phase (bottom) images of the same PZT Film using the nanopencil shown in (b). No inverted domains are observed after 10 V pulses were applied.

Figures 7a,b show cross-sectional mappings of the electric field component along the polarization axis, which drives domain nucleation, under the same bias conditions as in Figures 6c,d, i.e., 7 V for the 9 nm SWNT electrode and 10 V for the 3 nm one. The white areas correspond to electric field exceeding the experimental coercive field and are a measure of inverted domain volumes. We can see that the 9 nm electrode creates a concentrated electric field underneath it that is high enough to form a fully inverted polarization domain through the entire film thickness down to the grounded electrode (Figure 7a). On the other hand, only partial inversion switching occurs for 3 nm probe (Figure 7b). For the inverted domain to remain stable, the free energy reduction rate associated with the inverted domain has to be positive (Wang & Woo, 2003; Tayebi et al., 2010a). The energy reduction rate was predicted to be positive for the case of the 9 nm SWNT electrode (Tayebi et al., 2010a). This is due to the full polarization inversion over the entire PZT thickness, which reduces the surface area and volume over which the domain wall and depolarization forces are exerted. In this case the domain wall and depolarization forces are exerted only on the sides of the inverted domain compared to being through the entire domain. Therefore, the energy reduction induced by the coercive electric field will be larger than the surface energy of the domain wall.

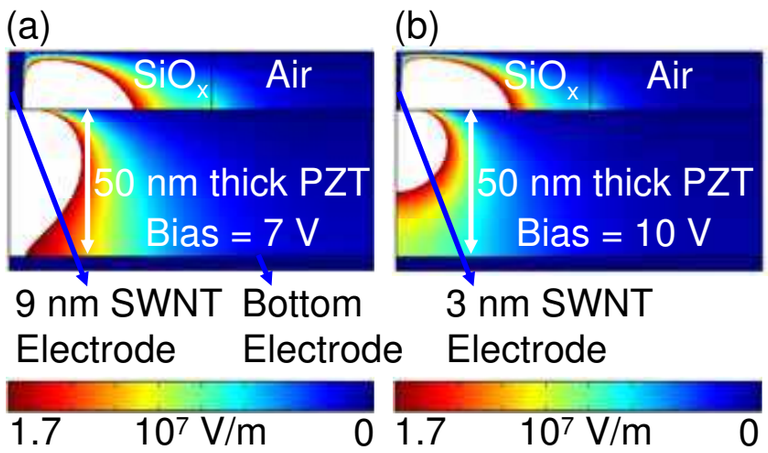

Fig. 7. (a), (b) Simulated cross-sectional mappings of the electric field component along the polarization axis under the same bias conditions of Figures 6c,d, i.e., 7 V for the 9 nm SWNT electrode (a) and 10 V for the 3 nm electrode (b) (Tayebi et al., 2010a). Due to the axial symmetry, only half of the system is shown. The white areas correspond to electric field exceeding the experimental coercive field and are a measure of inverted domain volumes.

On the other hand, the energy reduction rate was predicted to be negative for the case of the 3 nm SWNT electrode due to the partial polarization inversion (Tayebi et al., 2010a). To make the rate positive, the ferroelectric film had to be thinner to allow for full polarization inversion through the entire thicknees and therefore reduce the effects of the forces associated with domain wall and depolarization and built-in electric fields. Using a 17 nm thick PZT film, we were able to write stable 4 nm inverted domains that correpsond to 10 unit cells in size (Figure 8) (Tayebi et al., 2010a). If written in a checkerboard configuraton, densities as high as 40 Tbit/ in^2 can be achieved with such small domain sizes.

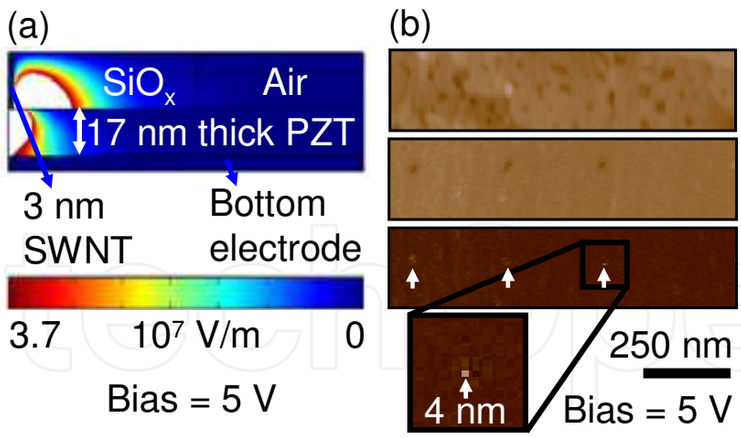

Fig. 8. Writing of stable 4 nm dots using 3 nm SWNT electrode on 17 nm thick PZT film (Tayebi et al., 2010a). (a) Simulated cross-sectional mappings of the electric field component along the polarization axis under a 5 V bias with a 3 nm SWNT electrode. Domain inversion through the entire film thickness is predicted. (b) PFM height (top), amplitude (middle) and phase (bottom) images of the 17 nm-thick PZT-film surface with 4 nm ferroelectric inverted domains formed by applying 5 V pulses to the film through the nanopencil with 3 nm electrode shown in Figure 6b.

Figure 9 depicts the minimum electrode size for predicted stable domain switching for various PZT thicknesses at different applied biases (properties of the 50 nm thick PZT film are assumed without a built-in field) (Tayebi et al., 2010a). For instance, the PZT film has to be thinner than 23 nm for a 3 nm electrode to write stable domains at 4 V bias pulses. Therefore, thinner ferroelectric films are required to enable formation of small stable domains at smaller applied biases. However, there is a critical film thickness limit below which the ferroelectric properties vanish (Junquera & Ghosez, 2003). This thickness has been estimated to be around 1.2–5 nm for both PZT (Despont et al., 2006; Fong et al., 2004; Lichtensteiger et al., 2007) and $BaTiO_3$ (Despont et al., 2006; Kim et al., 2005; Petraru et al., 2008) films. Recently, it was shown that highly strained $BaTiO_3$ films may retain their ferroelectric properties down to 1 nm thickness, i.e., below the critical thickness limit[6].

3.2 Tuning the built-in electric field

The stability of the sub-10 nm inverted domains can be further enhanced by reducing or even suppressing the built-in electric field, which is due to Pb vacancies near the surface. These vacancies are due to the high partial pressure of Pb atoms which can readily evaporate during deposition (Hau and Wong, 1995). A large remnant polarization can thus be induced, which is due to near surface concentration of trapped negative charges originating from this high vacancy density. The induced built-in electric field can exceed the coercive electric field needed for domain inversion. In such a case, stability of the inverted domains will be hard to achieve even if the forces due to depolarization charges and domain-walls are reduced. This is due to the fact that the built-in electric field is exerted over the same volume as the applied electric field, which might require a very large and impractical bias pulses to overcome the large remnant polarization. Note also that the built-in electric field is known to cause fatigue in FeRAM devices, and thus can dramatically affect the ferroelectric media lifetime (Miura & Tanaka, 1996).

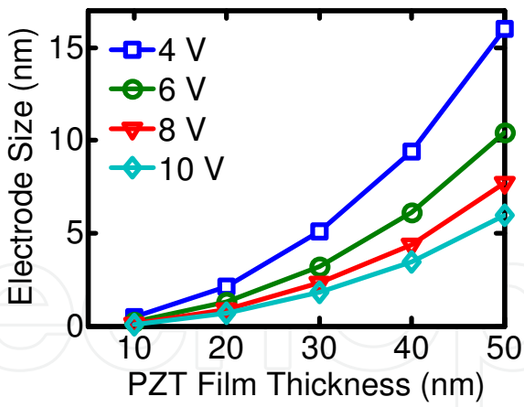

Fig. 9. Minimum electrode size for full-thickness domain inversions for various PZT thicknesses at different applied biases (Tayebi et al., 2010a).

The built-in electric-field can be tuned and suppressed by repetitive hydrogen (H_2) and oxygen (O_2) plasma treatments (Tayebit et al., submitted). Such treatments trigger reversible Pb reduction/ oxidation (redox) activity, thereby altering the electrochemistry of the Pb over-layer, which compensates for charges induced by the Pb vacancies. Figure 10 shows a set of the variation of the capacitance as a function of applied bias (C–V hysteresis loop curves) before (reference curve) and after various H_2 plasma treatments, in which the pressure was varied from 0.5 to 1 torr, while the flow rate was maintained at 1000 sccm (Tayebit et al., submitted). Under such oxygen poor conditions, reduction reaction of Pb film can extract O atoms from the PZT top surface and O vacancy formation is very stable (see next section). The positive charges induced from the formation of O vacancies compensate for the already existing negative charges induced by the Pb vacancies. This, in turn, reduces (case I: 0.5 Torr pressure condition) and even suppresses (case II: 1 Torr pressure condition) the built-in electric field, making the crosspoint at 0 V (initially at 0.25 V) (Tayebit et al., submitted).

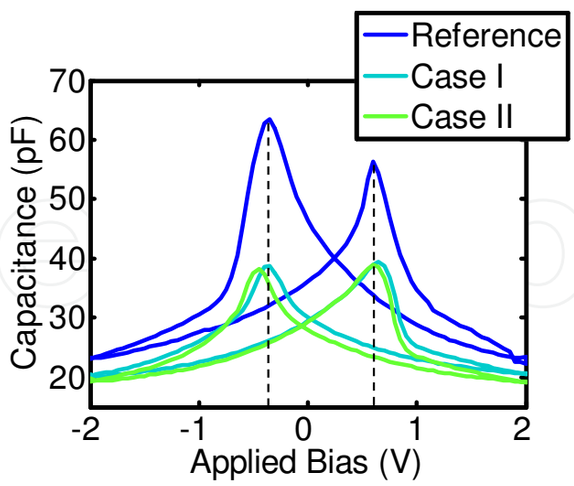

Fig. 10. Effect of the H_2 plasma treatments on the variation of capacitance as a function of applied bias. The built-in electric field decreases after each treatment, which is indicative of Pb reduction or O vacancy formation. The pressure was varied from 0.5 (case I) to 1 Torr (case II), while the gas flow rate of He with 4% H_2 was maintained at 1000 sccm (Tayebi et al., submitted).

Figure 11 shows the C–V hysteresis loop curves before (reference curve) and after the various O_2 plasma treatments, in which both pressure and gas rate where varied (Tayebit et al., submitted). Under such oxygen-rich conditions (see next section), the formation energies of O vacancies are highly positive and are thus unstable. The O_2 plasma treatments oxidize Pb in the PZT film, thereby filling the O vacancies that might have already existed in the film. This leads to an increase of negative charges induced by the Pb vacancies, which in turn shifts the C–V curve and hence increases the built-in electric field. Increasing the pressure and gas flow increases further the built-in electric field, thereby exacerbating its effect (case III to case IV).

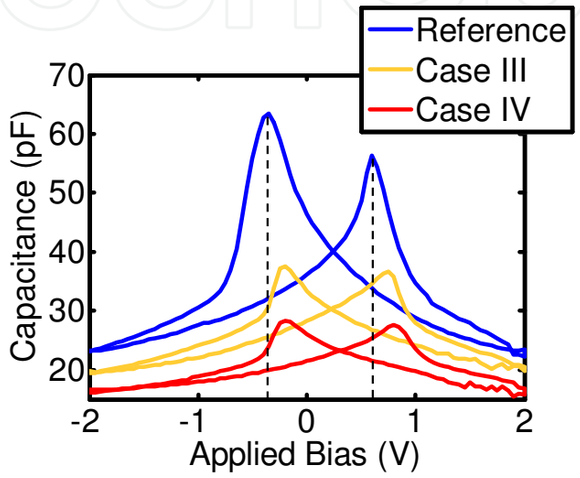

Fig. 11. Effect of the O2 plasma treatments on C–V hysteresis loop curve. The built-in electric field increases after each treatment, which is indicative of Pb oxidation or O vacancy filling. The O2 flow rate and pressure were varied from 100 sccm and 0.5 Torr (case III) to500 sccm and 5 Torr, respectively (Tayebi et al., submitted).

3.3 Review of a*b-Initio* studies of vacancy formation in PZT films

The formation of defects including lead vacancies $\left(V_{Pb}^{-2}\right)$ and O vacancies $\left(V_{O}^{+2}\right)$ under oxygen rich (oxidizing environment) and oxygen poor (reducing environment) has recently been investigated theoretically using *ab-initio* studies for $PbTiO_3$ (Zhukovskii et al., 2009; Zhang et al. 2006; Zhang et al., 2008) and $PbZrO_3$ (Zhukovskii et al., 2009). Note that $PbTiO_3$ and $PbZrO_3$ are the two systems that compose the PZT material. Moreover, besides Pb, Ti and Zr vacancies, there are two types of O vacancies that need to be taken into account. These correspond to O atoms bound to Ti/ Zr in the z direction referred to as O1, and O atoms bound to Ti/ Zr in x-y plane referred to as O2 (Figure 12). These calculations shed light on the charge compensation mechanism that enables the tuning of the built-in electric field and are thus reviewed here.

Figure 13a shows the variation of formation energies of various vacancies under oxygen-rich (oxidizing) conditions (Zhang et al. 2006). The formation energies of Pb vacancies are negative throughout the band gap of the PZT material. This confirms that the formation of Pb vacancies is an exothermic and spontaneous process that can happen during film growth. This is in agreement with our experimental observations where we attributed the origin of the built-in electric field and p-type conduction to the formation of Pb vacancies. On the other

hand, no O vacancies are stable given their highly positive formation energy. Therefore, under the oxygen rich conditions, the Pb vacancies cannot be compensated for. In fact, any O and Pb vacancies that might have been present will be filled by O atoms thereby oxidizing Pb. Such mechanism will exacerbate the effect of the built-in electric field and will increase the acceptor doping density. Note that Ti vacancies also possess very highly positive formation energies and are not susceptible to form. Although not shown in Figure 13a, this is also the case of Zr as reported in other *ab-initio* studies (Zhukovskii et al., 2009).

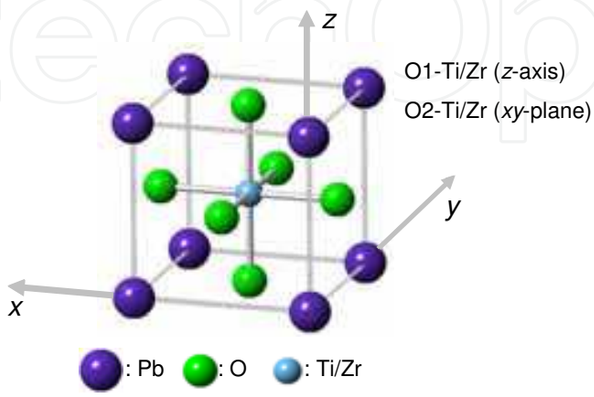

Fig. 12. PZT unit cell depicting the two types of O atoms. O atoms bound to Ti/ Zr in the z direction are referred to as O1, and O atoms bound to Ti/ Zr in x-y plane are referred to as O2.

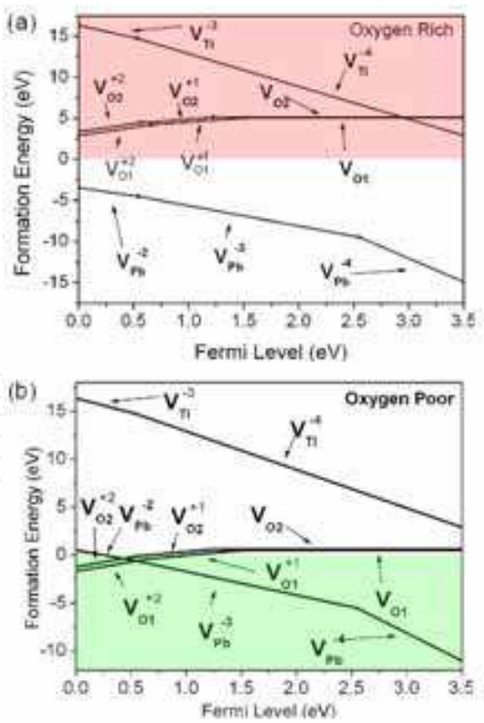

Fig. 13. Previously published *ab-initio* calculations of defect formation energy for vacancies as a function of the Fermi level in oxygen-rich (a) and oxygen-poor (b) conditions (Zhang et al., 2006). Only the vacancies among the lowest formation energies are shown.

On the other hand, both O and Pb vacancies possess negative formation energies under the oxygen-poor (reducing) conditions, as shown in Figure 13b (Zhang et al., 2006). Therefore both vacancies are susceptible to form under these conditions. Moreover, the V_O^{+2} vacancy possesses even lower formation energy than V_{Pb}^{-2} at the same Fermi level, and is thus more stable. Therefore, the large density of the O vacancies under oxygen poor conditions will affect the initial *p*-type conductivity of the PZT film. It will also reduce, suppress or even change the direction of the built-in electric field if the O vacancies exceed the Pb ones.

4. Probe-based reading techniques

A few conventional probe-based reading techniques have been developed and that are capable of detecting polarization bit signals at the required high scanning speeds on the order of mm/ s which are required for high data access rates (Nath et al., 2008; Hiranaga et al., 2007; Park et al., 2004). However, not all techniques are suitable for a MEMS-based probe storage system. For example, piezoresponse force microscopy (PFM) (Tybell et al., 1998; Hong et al., 2002; Kalinin et al., 2004; Nath et al., 2008) uses an opto-electro-mechanical setup to detect high-frequency piezoactuation signals while scanning without active tracking of surface to achieve high-speed imaging of local polarizations (Nath et al., 2008). This is achieved by measuring the mechanical response of the ferroelectric film when an AC voltage is superimposed to the surface during scanning. In response to the electrical stimulus (inverse piezoelectric effect), the film locally expands or contracts inducing a deflection of the probe-cantilever, which is measured using a split photodiode detector, which is then demodulated. The piezoelectric response of the sample is the first harmonic component of the bias induced tip deflection z. When a bias $V = V_{DC} + V_{AC}\cos(\omega t)$ is applied to the probe-tip, the resulting cantilever deflection $z = z_{DC} + A(\omega, V_{DC}, V_{AC})\cos(\omega t + \phi)$, where A and φ are the amplitude and phase of the electromechanical response, respectively. For down polarized domains, the application of a positive tip-bias results in sample expansion, and surface oscillations are in phase with the applied bias, i.e., $\varphi = 0$. On the other hand, the surface oscillations are out of phase with the applied bias for up polarized domain, and the phase is shifted by 180°. There are other techniques that are exclusively electrically-based such as scanning nonlinear dielectric (Hiranaga et al., 2007) and scanning resistive probe (Park et al., 2004) microscopy techniques. However, these two techniques require complex configurations such as the use of a coaxial tip geometry to allow for fast reading of capacitance changes associated with polarization domain signals, and field effect sensors integrated at the tip apex, respectively.

Recently, a technique called charge-based scanning probe read-back microscopy has been developed (Forrester et al, 2009). In this technique, ferroelectric inverted domains are read back destructively by applying a constant voltage of magnitude greater than the coercive voltage needed for polarization reversal. This is similar to FeRAM-based reading mechanism. In this process, the flow of screening charges through the read-back amplifier provides sufficient signal to enable the read of inverted domains as small as 10 nm with frequencies read-back at rates as high as 1.5 MHz and speeds as high as 2 cm/ s, which is much faster than other developed techniques. Figure 14 shows the reading mechanism used in this technique. During scanning, a constant voltage is applied between the moving tip and the bottom electrode on which the ferroelectric film is deposited. This in turn causes

inverted domains whose polarization direction is anti-parallel to the applied electric field to invert back. This causes the bound charge at the top and bottom surfaces to reverse and thus the surface screening charges also reverse. The resulting charge flow can be detected by a charge- or current-sensitive amplifier. Knowing what the film polarization is, the inverted domain area can be determined from the detected charge signal. Figure 15 shows a read-back signal for a single tone pattern of inverted domains in which switching and non-switching signals are resolved with high signal-to-noise ratio. The main disadvantage of this technique, however, is that the reading is destructive and requires immediate rewriting of bits, which can cause rewriting inaccuracies from probe registry offsets. It can also induce slower access rates.

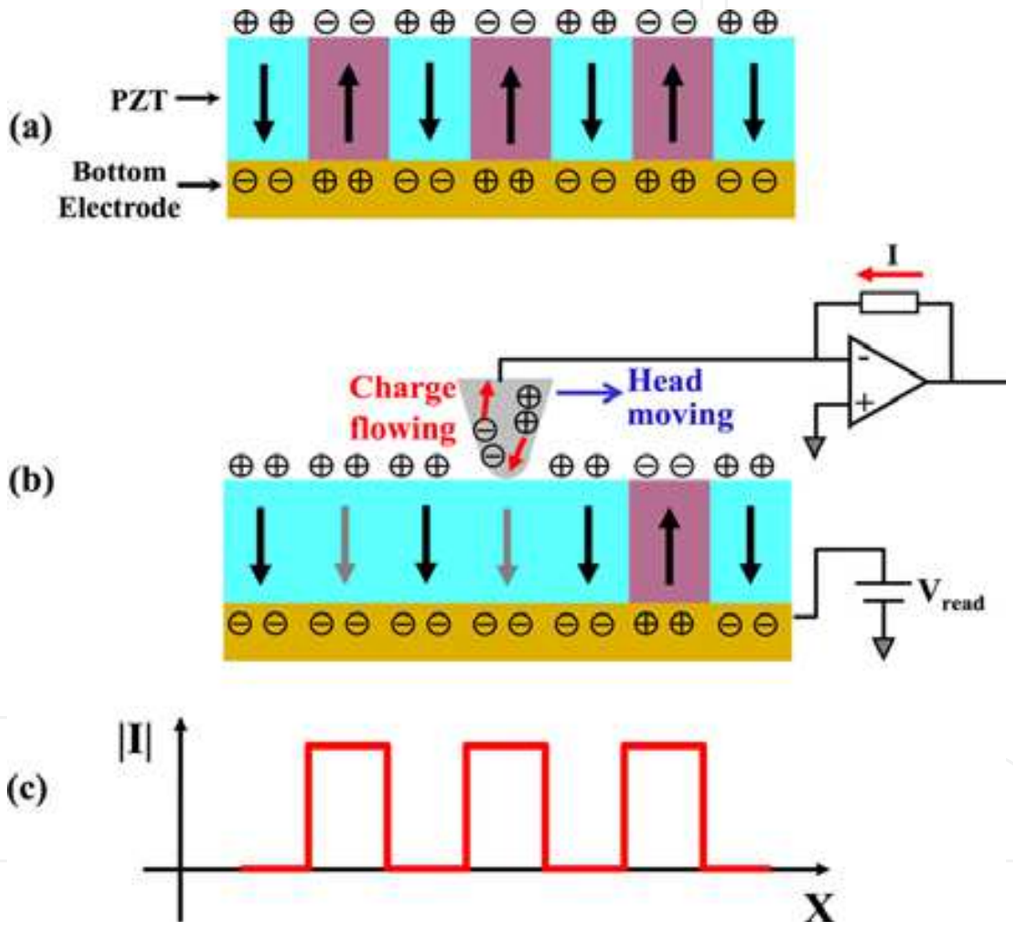

Fig. 14. Schematic drawing of the ferroelectric read-back process (Forrester et al., 2009). (a) A domain pattern of alternating up and down polarizations. The circled symbols represent screening charges which compensate the bound charges associated with each polarization. (b) During read-back a constant voltage is applied between the probe tip and the base electrode causes reversal (erasing) of domains whose polarization is opposite to the applied electric field. The resulting flow of screening charges is sensed by the read-back amplifier, producing a read-back signal that is schematically shown in (c).

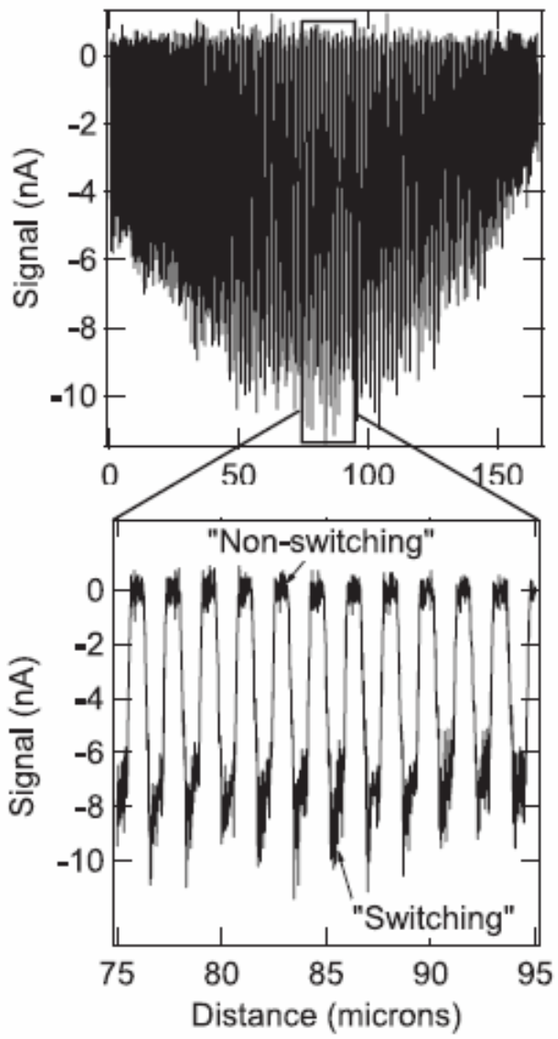

Fig. 15. Read-back data of a 800 nm bit length, showing an entire 170 μm track (Forrester et al., 2009).

Another recently developed technique, which has the advantage of using a nondestructive read process, is the scanning probe charge reading technique (Kim et al., 2009). Unlike the PFM technique, this technique uses the direct piezoelectric effect. The applied normal force excreted by the probe-tip during scanning causes a charge buildup Q related to the force by the equation $Q=d_{33}F$, where d_{33} is a piezoelectric coefficient of the ferroelectric medium along the polarization access. Therefore, a current is generated due to a change in charge when the probe tip crosses a domain wall of the inverted domain. The sign of the current depends on whether the probe tip moves from an up to down polarization or vice versa. Figure 16 shows a schematic of the operational principle of this technique in which a series of inverted domains written with wavelength λ are read using this technique. By converting the charge coupled to the probe tip from the ferroelectric film into an output voltage, the desired alternating polarization charges are read. The voltage signal is fed through a band- pass filter to generate a cleaner signal, V_{BPF}.

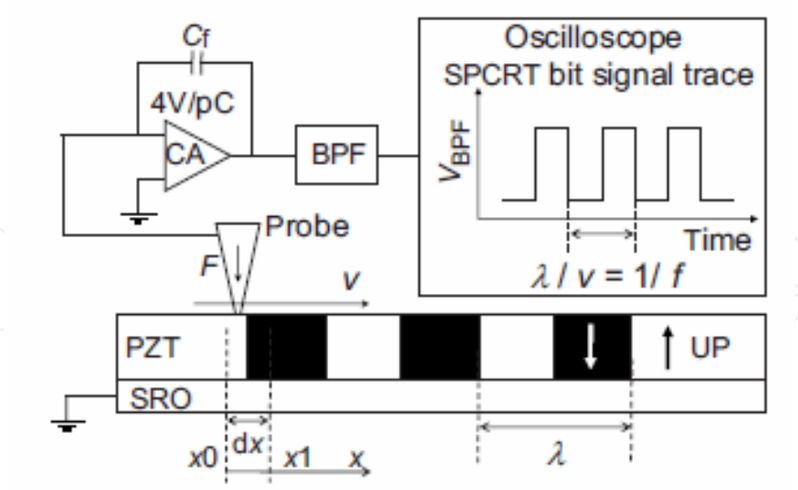

Fig. 16. Schematic drawing of the principle of operation and a test setup of the scanning probe charge reading technique to read ferroelectric bits (Kim et al., 2009).

Figure 17 shows a set of voltage signal traces corresponding to three inverted-domain wavelengths: 1.6, 1.2, and 0.8 μm, respectively and for various applied forces at a scanning speed of 1.6 mm/ s. The signal-to-noise ratio for the three wavelengths increases from 14, 12, and 10 dB to 17, 15, and 13 dB as the applied force is increased from 100 nN to 800 nN. When the probe tip is disengaged no discernable signal is detected.

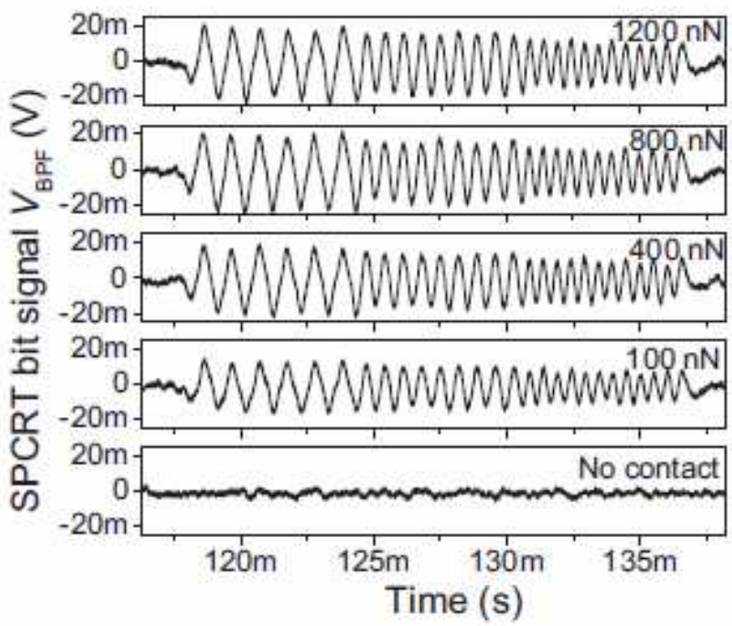

Fig. 17. Bit signal traces in time domain of the three different wavelengths (1.6, 1.2, and 0.8 μm), alternating polarizations at various applied forces. The scanning speed was maintained at 1.6 mm/ s (Kim et al., 2009).

5. A 5 kilometer tip-wear endurance mechanism

For probe-based memory devices to be technologically competitive, the write and read operations have to be achieved at high access rates with sliding velocities on the order of 5 to 10 mm/ s, over a lifetime of 5 to 10 years, corresponding to probe-tip sliding distances of 5 to 10 km. The bit size, and thus the storage density, mainly depends on the radius of the probe-tip, which is prone to rapid mechanical wear and dulling due to the high-speed contact mode operation of the system (Cho et al., 2006; Knoll et al., 2006; Bhushan et al., 2008; Gotsmann & Lantz, 2008). This tip wear can cause serious degradation of the write-read resolution over the device lifetime and remains the most important fundamental issue facing probe-based storage.

In principle, the tip wear rate could be reduced by using hard conductive diamond coatings (Cho et al., 2006). However, such coatings are usually deposited at high temperatures (~900^{o}C), which are not compatible with integration processes of on-chip electronic circuits (Heck et al., 2010). The diamond coatings are also very rough and have to be sharpened by focus ion beam schemes to reduce the tip radius in order to achieve the required write-read resolution (Cho et al., 2006), which make it difficult for large scale batch fabrication of probe arrays (Heck et al., 2010). Carbon nanotube probe-tips, which due to their cylindrical shape can retain their write-read resolution even after significant wear, have also been proposed. These include "naked" carbon nanotube probes (Lantz et al., 2003) and the dielectric-sheathed carbon nanotube probes presented in section 3 (Tayebi et al., 2010a). It will, however, take a significant time and research effort to bring such probes to large scale fabrication (Heck et al., 2010). Thus conventional conductive coatings with small tip radius that can be deposited at ambient or low temperature conditions, such as platinum-iridium (PtIr), remain the best choice at the present time.

Our group has developed a scheme for a wear endurance mechanism which allows a conductive PtIr coated probe-tip sliding over a ferroelectric film at a 5 mm/ s velocity to retain its write-read resolution over a 5 km distance, which corresponds to a 5 year device lifetime (Tayebi et al., 2010b). This mechanism was achieved by sliding the probe-tip at low applied forces on atomically smooth surfaces with force modulation and in the presence of thin water films under optimized humidity. Under the conditions of low applied forces on atomically smooth surfaces, the adhesive elastic wear regime is dominant, whereas the abrasive wear regime encountered in rough contact is significantly reduced. This in turn reduces the wear rate by orders of magnitude. In the elastic wear regime, the wear volume is inversely dependent on the elastic modulus of the coating rather than its hardness (Bhushan, 2002).

Modulating the force in the presence of an ultrathin water layer, which acts as a viscoelastic film, further reduced the wear volume to insignificant amounts. This is because force modulation enables the probe-tip to recover elastically during sliding every time the nominal force is reduced during a modulation cycle. This in turn would relax the stress level on bonds between atoms that are taking part in the wear process, delay bond breaking, and thus reduce wear. Furthermore, the insertion of the ultrathin water film that is a few monolayers in thickness at the tip-sample interface provides further wear rate reduction. Such a thin film strongly adheres to the surface, thus forming a liquid crystal, and is not energetically favored to form a meniscus at the tip-sample interface.

Under force modulation of high frequency, this water film can act as a viscoelastic material, which would further reduce the stress level on such bonds and decrease friction and wear.

Figures 18b,c show SEM images of the PtIr probe-tip after 2.5 km and 5 km sliding distances (corresponding to two weeks of continuous sliding) under the conditions mentioned above. The wear volume is estimated to be 3.32×10^3 nm^3 after 2.5 km and 5.6×10^3 nm^3 after 5 km. Figures 18d,e show a 3×1 matrix of inverted domain dots written by applying 100 μs wide pulses of 5V before and after 5 km sliding, with the same domain sizes of 15.6 nm. Although the tip has shown a small amount of wear, the write and read resolutions were therefore not lost after 5 km of sliding at 5 mm/ s.

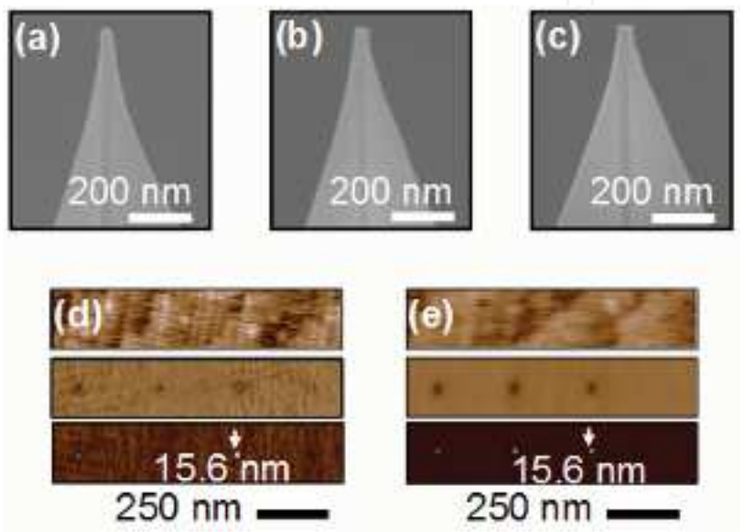

Fig. 18. Wear tests on PtIr probe-tips sliding over a PZT surface with 0.17 nm RMS roughness with force modulation and water lubrication (Tayebi et al., 2010b). (a-c) SEM images of as received PtIr probe-tip prior to sliding (a), after 2.5 km (b) and 5 km (c) of sliding at 5 mm/ s with an applied normal force F_N = 7.5 nN that is modulated at 200 kHz. (d, e) PFM height (top), amplitude (middle) and phase (bottom) images of the PZT-film surface with 3×1 matrix of 15.6 nm inverted domains formed by applying 100 μs pulses of 5 V using the probe-tip prior to (d) and after (e) the 5 km sliding experiment.

On the other hand, sliding experiments performed without force modulation while keeping other conditions identical including the 25% RH level, showed a significant tip blunting after only 500 m sliding with a tip wear volume of 8.2×10^5 nm^3 (Figures 19a,b). Figures 19c,d show a 4×1 matrix of inverted domain dots written by applying 100 μs wide pulses of 5V before and after the 500 m sliding. Here the dot size increased by 31.4 nm from the as-received tip conditions. Therefore sliding under force modulation within the elastic adhesive wear regime and in the presence of a thin water layer greatly reduces wear. These results could lead to parallel-probe based data storage devices that exceed the capabilities of current hard drive and solid state disks given the ultrahigh density capabilities. It can also allow other scanning probe based systems such as AFM-based lithograph.

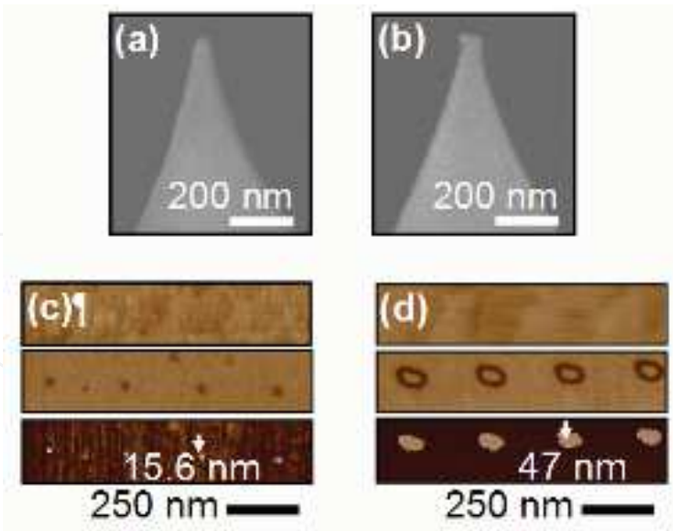

Fig. 19. Wear tests on PtIr probe-tips sliding over a PZT surface with 0.17 nm RMS roughness without force modulation (Tayebi et al., 2010b). (a, b) SEM images of another PtIr probe-tip prior (a) and after 500 m (b) of sliding at 5 mm/ s with an applied normal force F_N = 7.5 nN without force modulation. (c) Height (top), amplitude (middle) and phase (bottom) images of the film surface with 4×1 matrix of 15.6 nm inverted domains formed under the same conditions using the PtIr probe-tip prior to the 500 m sliding experiment without modulation. (d) Height (top), amplitude (middle) and phase (bottom) images of the film surface with 4×1 matrix of 47 nm inverted domains formed under the same conditions after the 500 m sliding experiment. The size of the inverted domains increased by 31.2 nm after sliding.

6. Conclusions

This chapter reviewed recent progress to address several fundamental issues that have remained a bottleneck for the development and commercialization of ultrahigh density probe-based nonvolatile memory devices using ferroelectric media, including stability of sub-10 nm inverted ferroelectric domains, reading schemes at high operating speeds compatible with MEMS-based storage systems, and probe-tip wear.

Stable inverted domains less than 10 nm in diameter could be formed in ferroelectric films when inversion occurred through the entire ferroelectric film thickness. Polarization inversion was found to depend strongly on the ratio of the electrode size to the ferroelectric film thickness. This is because full inversion minimized the effects of domain-wall and depolarization energies by reducing the domain sidewalls and, thus enabling positive free energy reduction rates. With this understanding, stable inverted domains as small as 4 nm in diameter were experimentally demonstrated. Moreover, the reduction and suppression of the built-in electric field, which would enhance the stability of sub-10 nm domains in up and down-polarized ferroelectric PZT films, could be achieved by repetetive O_2 and H_2 plasma treatments to oxidize/ reduce the PZT surface, thereby altering the electrochemistry of the Pb over-layer. These treatments compensate for the negative charges induced by the Pb vacancies that are at the origin of the built-in electric field.

Two probe-based reading techniques have shown potential compatibility with MEMS-based probe storage systems at high speed rates: the charge-based scanning probe and the

scanning probe charge reading techniques. In the charge-based scanning probe read-back microscopy, ferroelectric inverted domains are read back destructively by applying a constant voltage that is greater than the coercive voltage of the ferroelectric film. In this process, the flow of screening charges through the read-back amplifier provides sufficient signal to enable the read of inverted domains as small as 10 nm with frequencies read-back at rates as high as 1.5 MHz and speeds as high as 2 cm/ s. For the case of the scanning probe charge reading technique, the direct piezoelectric effect is used. The applied normal force excreted by the probe-tip during scanning causes a charge buildup, which generates a current when the probe tip travels across a domain wall of the inverted domain. Besides reading at high speeds, this technique has the advantage of being nondestructive.

Lastly, we discussed a wear endurance mechanism which enabled a conductive PtIr coated probe-tip sliding over a ferroelectric film at a 5 mm/ s velocity to retain its write-read resolution over a 5 km distance, corresponding to 5 years of device lifetime. This was achieved by sliding the probe-tip at low applied forces on atomically smooth surfaces, with force modulation, and in the presence of thin water films under optimized humidity. Under the conditions of low applied forces on atomically smooth surfaces, the adhesive elastic wear regime was dominant, and the wear rate was reduced by orders of magnitude. In this regime, the wear volume is inversely dependent on the elastic modulus of the coating rather than its hardness. Modulating the force in the presence of a thin water layer, which acts as a viscoelastic film, further reduced the wear volume to insignificant amounts.

The novel solutions summarized in this chapter could lead to parallel-probe based data storage devices that exceed the capabilities of current hard drive and solid state disks given the ultrahigh density capabilities this technology possesses. While fundamental issues have been addressed, the solutions were obtained at the single probe level. Therefore, these solutions have to be tested and validated in actual devices, such as the Intel's SSP memory device (Heck et al., 2010) where 5000 MEMS cantilever-probes can simultaneously perform write and read operations.

7. References

Ahn, C. H., Tybell, T., Antognazza, L., Char, K.; Hammond, R. H., Beasley, M. R.; Fischer, Ø., and Triscone J-M. (1997). Nonvolatile electronic writing of epitaxial $Pb(Zr_{0.52}Ti_{0.48})O_3$/ $SrRuO_3$ heterostructures, *Science*, Vol. 276, pp. 1100.

Ahn, C. H., Rabe, M. R., and Triscone, J-M. (2004). Ferroelectricity at the nanoscale: Local polarization in oxide thin films and heterostructures, *Science*, Vol. 303, pp. 488.

Bhushan, B., Kwak, K. J., and Palacio, M. (2008). Nanotribology and nanomechanics of AFM probe-based data recording technology, *Journal of Physics: Condensed Matter*, Vol. 20, pp. 365207.

Bhushan, B. (2002). *Introduction to Tribology.* New York, NY. John Wiley & Sons.

Cho, Y., Fujimoto, K., Hiranaga, Y., Wagatsuma, Y., Onoe, A., Terabe, K., and Kitamura, K. (2003). Terabit/ inch^2 ferroelectric data storage using scanning nonlinear dielectric microscopy nanodomain engineering system, *Nanotechnology,* Vol. 14, pp. 637.

Cho, Y., Hashimoto, S., Odagawa, N., Tanaka, K., and Hiranaga, Y. (2005). Realization of 10 Tbit/ in^2 memory density and subnanosecond domain switching time in ferroelectric data storage, *Applied Physics Letters* Vol. 87, pp. 232907.

Cho, Y., Hashimoto, S., Odagawa, N., Tanaka, K., and Hiranaga, Y. (2006). Nanodomain manipulation for ultrahigh density ferroelectric data storage, *Nanotechnology,* Vol. 17, pp. S137.

Despont, L., Koitzsch, C., Clerc, F.; Garnier, M. G., Aebi, P., Lichtensteiger, C., Triscone, J.-M., Garcia de Abajo, F. J., Bousquet, E. and Ghosez, Ph. (2006). Direct evidence for ferroelectric polar distortion in ultrathin lead titanate perovskite films, *Physical Review B*, Vol. 73, pp. 094110.

Fong, D. D., Stephenson, G. B., Streiffer, S. K., Eastman, J. A., Auciello, O., Fuoss, P. H. and Thompson, C. (2004). Ferroelectricity in ultrathin perovskite films, *Science*, Vol. 304, pp. 1650.

Forrester, M. G., Ahner, J. W., Bedillion, M. D., Bedoya, C., Bolten, D. G., Chang, K-C, de Gersem, G., Hu, S., Johns, E. C., Nassirou, M., Palmer, J., Roelofs, A., Siegert, M., Tamaru, S., Vaithyanathan, V., Zavaliche, F., Zhao, T., and Zhao Y. (2009). Charge-based scanning probe readback of nanometer-scale ferroelectric domain patterns at megahertz rates, *Nanotechnology* Vol. 20,pp. 225501.

Garcia, V., Fusil, S., Bouzehouane, K., Enouz-Vedrenne, S., Mathur, N. D., Barthélémy, A. and Bibes, M. (2009). Giant tunnel electroresistance for non-destructive readout of ferroelectric states, *Nature*, Vol. 460, pp. 81.

Gotsmann, B. and Lantz, M. A. (2008). Atomistic wear in a single asperity sliding contact, *Physical Review Letters,* Vol. 101, pp. 125501.

Hamann, H., O'Boyle, M., Martin, Y. C., Rooks, M., and Wickramasinghe, H. K. (2006). Ultra-high-density phase-change storage and memory, *Nature Materials,* Vol. 5, pp. 383.

Hau, S.K. and Wong, K.H. (1995). Intrinsic resputtering in pulsed–laser deposition of lead–zirconate–titanate thin films, *Applied Physics Letters*, Vol. 66, pp. 245.

Heck, J., Adams, D., Belov, N., Chou, T. A., Kim, B., Kornelsen, K., Ma, Q., Rao, V., Severi, S., Spicer, D., Tchelepi, G. and Witvrouw, A. (2010). Ultra-high density MEMS probe memory device, *Microelectronic Engineering*, Vol. 87, pp. 1198.

Hiranaga, Y., Uda, T. Kurihashi, Y., Tanaka, K. and Cho, Y. (2007). Novel HDD-type SNDM ferroelectric data storage system aimed at high-speed data transfer with single probe operation. *IEEE Transanctions on Ultrasonnics,.Ferroelectrics and Frequency Control*, Vol. 54, pp. 2523.

Junquera, J. and Ghosez, P. (2003). Critical thickness for ferroelectricity in perovskite ultrathin films, *Nature*, Vol. 422, pp. 506.

Hong, S., Shin, H., Woo, J. and No, K. (2002). *Effect of cantilever–sample interaction on piezoelectric force microscopy*, *Applied Physics Letters,* Vol. 80, pp. 1453

Kalinin, V., Karapetian, E. and Kachanov, M. (2004). Nanoelectromechanics of piezoresponse force microscopy, *Physical Review B,* Vol. 70, pp. 184101.

Kim, B. M, Adams, D. E., Tran, Q., Ma, Q. and Rao, V. (2009). Scanning probe charge reading of ferroelectric domains, *Applied Physics Letters*, Vol. 94, pp. 063105.

Kim, D. J., Jo, J. Y., Kim, Y. S., Chang, Y. J., Lee, J. S., Yoon, J. G., Song, T. K. and Noh, T. W. (2005). Polarization relaxation induced by a depolarization field in ultrathin ferroelectric $BaTiO_3$ capacitors, *Physical Review Letters*, Vol. 95, pp. 237602.

Knoll, A., Bächtold, P., Bonan, J., Cherubini, G., Despont, M., Drechsler, U., Dürig, U., Gotsmann, B., Häberle, W., Hagleitner, C., Jubin, D., Lantz, M.A., Pantazi, A., Pozidis, H., Rothuizen, H., Sebastian, A., Stutz, R., Vettiger, P., Wiesmann D. and

Eleftheriou, E.S. (2006). Integrating nanotechnology into a working storage device," *Microelectronics Engineering,* Vol. 83, pp. 1692.

Kim, Y. S ., Kim, D. H., Kim, J. D., Chang, Y. J., Noh, T. W., Kong, J. H., Char, K., Park, Y. D., Bu, S. D., Yoon, J.-G. and Chung, J.-S. (2005). Critical thickness of ultrathin ferroelectric $BaTiO_3$ films, *Applied Physics Letter*s, Vol. 86, pp. 102907.

Lantz, M. A., Gotsmann, B., Durig, U. T., Vettiger, P., Nakayama, Y., Shimizu, T. and Tokumoto, H. (2003). Carbon nanotube tips for thermomechanical data storage, *Applied Physics Letter,* Vol. 83, pp. 1266.

Lichtensteiger, C., Dawber, M., Stucki, N., Triscone, J.-M., Hoffman, J., Yau, J.-B., Ahn, C. H., Despont, L. and Aebi, P. (2007). Monodomain to polydomain transition in ferroelectric $PbTiO_3$ thin films with $La_{0.67}Sr_{0.33}MnO_3$ electrodes, *Applied Physics Letters*, Vol. 90, pp. 052907.

Li, X., Mamchik, A. and Chen, I.-W. (2001). Stability of electrodeless ferroelectric domains near a ferroelectric dielectric interface, *Applied Physics Letters,* Vol. 79, pp. 809.

Miura, K. and Tanaka M, (1996). Origin of Fatigue in Ferroelectric Perovskite Oxides, *Japanese Journal of Applied Physics*, Vol. 35, pp. 2719.

Nath, R., Chu, Y. –H, Polomoff, N. A., Ramesh, R., and Huey, B. D. (2008). High speed piezoresponse force microscopy: <1 frame per second nanoscale imaging, *Applied Physics Letters*, Vol. 93, pp. 072905.

Pantazi, A., Sebastian, A., Antonakopoulos, T. A., Bächtold, P., Bonaccio, A. R., Bonan, J., Cherubini, G., Despont, M., DiPietro, R. A., Drechsler, U., Dürig, U., Gotsmann, B., Häberle, W., Hagleitner, C., Hedrick, J. L., Jubin, D., Knoll, A., Lantz, M. A., Pentarakis, J., Pozidis, H., Pratt, R. C., Rothuizen, H., Stutz, R., Varsamou, M., Wiesmann, D., and Eleftheriou, E., (2008). Probe-based ultrahigh-density storage technology, *IBM Journal of Research and Development, Vol. 52*, pp. 493.

Park, H., Jung, J., Min, D. -K., Kim, S., Hong, S. and Shin, H. (2004). Scanning resistive probe microscopy: Imaging ferroelectric domains. *Applied Physics Letters,* Vol. 84, pp. 1734.

Petraru, A., Kohlstedt, H., Poppe, U., Waser, R., Solbach, A., Klemradt, U., Schubert, J., Zander, W. and Pertsev, N. A. (2008). Wedgelike ultrathin epitaxial $BaTiO_3$ films for studies of scaling effects in ferroelectrics, *Applied Physics Letters*, Vol. 93, pp. 072902.

Tayebi, N., Nauru, Y., Franklin, N., Collier, C. P., Giapis, K. P., Nishi, N., and Zhang, Y. (2010). Fully Inverted Single-Digit Nanometer Domains in Ferroelectric Films, *Applied Physics Letters*, Vol. 96, No. 2, pp. 023103.

Tayebi, N., Narui, Y., Chen, R. J., Collier, C. P., Giapis, K. P., and Zhang, Y. (2008a). Nanopencil as a Wear-Tolerant Probe for Ultrahigh Density Data Storage, Applied Physics Letters, Vol. 93, No. 10, pp. 103112.

Tayebi, N., Zhang, Y., Chen, R. J., Tran, Q., Chen, R., Ma, Q., Nishi, Y., and Rao, V. (2010b) An Ultraclean Tip-Wear Reduction Scheme for Ultrahigh Density Scanning Probe-Based Data Storage, *ACS NANO,* Vol. 4, No. 10, pp. 5713-20.

Tayebi, N., Kim, S., Franklin, N., Chen, R..J., Tran, Q., Ma, Q., Nishi, Y., and Rao, V. (submitted). Tuning and Suppression of Built-in Electric Field for Long Term Retention of Single-Digit Nanometer Domains in Ferroelectric Films.

Tybell, T., Ahn, C. H. and Triscone, J. -M. (1998). Control and imaging of ferroelectric domains over large areas with nanometer resolution in atomically smooth epitaxial Pb(Zr0.2Ti0.8)O3 thin films. *Applied Physics Letters*, Vol. 72, pp. 1454.

Vettiger, P., Cross, G., Despont, M., Drechsler, U., Dürig, U., Gotsmann, B., Häberle, W., Lantz, M. A., Rothuizen, H. E., Stutz, R., and Binnig G. K. (2002). The 'Millipede' – Nanotechnology entering data storage, *IEEE Transactions on Nanotechnology*, Vol. 1, pp.

Wang, B. and Woo, C.H. (2003). Stability of 180° domain in ferroelectric thin films, *Journal of Applied Physics*, Vol. 94, pp. 610.

Zhang, Z., Wu, P., Lu, L. and Shu, C. (2006). Study on vacancy formation in ferroelectric $PbTiO_3$ from *ab initio*, *Applied Physics Letters* Vol. 88, pp. 142902.

Zhang, Z., Wu, P., Lu, L. and Shu, C. (2008). *Ab initio* study of formations of neutral vacancies in ferroelectric $PbTiO_3$ at different oxygen atmospheres, *Journal of Alloys and Compounds Vol. 449*, pp. 362.

Zhukovskii, Y. F., Kotominb, E. A., Piskunov, S. and Ellis, D.E., (2009). A comparative *ab initio* study of bulk and surface oxygen vacancies in $PbTiO_3$, $PbZrO_3$ and $SrTiO_3$ perovskites, *Solid State Communications,* Vol. 149, pp. 1359.

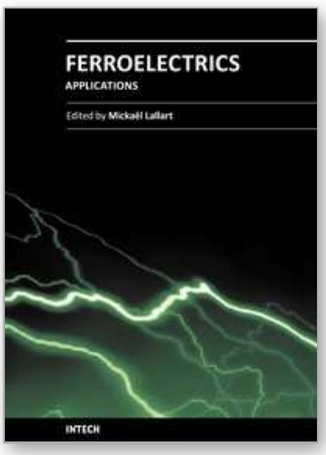

Ferroelectrics - Applications
Edited by Dr. MickaÃ«l Lallart

ISBN 978-953-307-456-6
Hard cover, 250 pages
Publisher InTech
Published online 23, August, 2011
Published in print edition August, 2011

Ferroelectric materials have been and still are widely used in many applications, that have moved from sonar towards breakthrough technologies such as memories or optical devices. This book is a part of a four volume collection (covering material aspects, physical effects, characterization and modeling, and applications) and focuses on the application of ferroelectric devices to innovative systems. In particular, the use of these materials as varying capacitors, gyroscope, acoustics sensors and actuators, microgenerators and memory devices will be exposed, providing an up-to-date review of recent scientific findings and recent advances in the field of ferroelectric devices.

How to reference
In order to correctly reference this scholarly work, feel free to copy and paste the following:

Noureddine Tayebi and Yuegang Zhang (2011). Ultrahigh Density Probe-based Storage Using Ferroelectric Thin Films, Ferroelectrics - Applications, Dr. MickaÃ«l Lallart (Ed.), ISBN: 978-953-307-456-6, InTech, Available from: http://www.intechopen.com/books/ferroelectrics-applications/ultrahigh-density-probe-based-storage-using-ferroelectric-thin-films

INTECH
open science | open minds

InTech Europe
University Campus STeP Ri
Slavka Krautzeka 83/A
51000 Rijeka, Croatia
Phone: +385 (51) 770 447
Fax: +385 (51) 686 166
www.intechopen.com

InTech China
Unit 405, Office Block, Hotel Equatorial Shanghai
No.65, Yan An Road (West), Shanghai, 200040, China
中国上海市延安西路65号上海国际贵都大饭店办公楼405单元
Phone: +86-21-62489820
Fax: +86-21-62489821

IntechOpen